

Published in final edited form as:

Retina. 2014 May ; 34(5): 989–995. doi:10.1097/IAE.000000000000022.

Association of Dark-Adapted Visual Function with Retinal Structural Changes in Patients with Stargardt Disease

Serena Salvatore, MD^{(1),(2)}, Gerald A. Fishman, MD^{(2),(3)}, J. Jason McAnany, PhD⁽³⁾, and Mohamed A. Genead, MD⁽²⁾

⁽¹⁾Department of Ophthalmology, University La Sapienza of Rome, Polo Pontino, Latina, Italy

⁽²⁾Pangere Center for Hereditary Retinal Diseases, The Chicago Lighthouse for People Who Are Blind or Visually Impaired, Chicago, Illinois, USA

⁽³⁾Department of Ophthalmology and Visual Science, University of Illinois at Chicago, Chicago, Illinois, USA

Abstract

Purpose—To evaluate dark-adapted retinal sensitivity in patients with Stargardt disease (STGD1) using a modified MP-1 microperimeter (MP-1S) and to compare the sensitivity loss with structural changes observed by spectral-domain optical coherence tomography (SD-OCT) and confocal scanning laser ophthalmoscope (cSLO) infrared imaging.

Methods—Twelve STGD1 patients and 10 normally sighted controls participated. Dark-adapted mean sensitivity (MS) was obtained using a MP-1S. Additionally, MS percent difference between the patients and the controls was obtained. Sensitivity results were superimposed on cSLO infrared images and compared with corresponding SD-OCT scans.

Results—Dark-adapted $MS \pm SD$ was 8.34 ± 1.54 dB for the controls and 3.68 ± 1.74 dB for STGD1 ($p < 0.001$). There was a significant reduction in MS of 24.0% in STGD1. Sensitivity reductions were observed in areas that showed changes on cSLO infrared images and on SD-OCT, including disorganizational loss of the retinal pigment epithelium, and abnormal photoreceptor inner-segment ellipsoid (ISe) and external limiting membrane reflectance band.

Conclusions—With topographical accuracy, dark-adapted sensitivity measurements can be made in STGD1 and normal controls with the MP-1S. Sensitivity loss is associated with structural changes. This finding can be useful for the determination of optimal areas for potential improvement of retinal function in Stargardt patients.

Keywords

confocal scanning laser ophthalmoscope infrared imaging; dark-adapted retinal sensitivity; fundus-related perimetry; spectral-domain optical coherence tomography; Stargardt disease

Corresponding Author: Gerald A. Fishman, MD, The Chicago Lighthouse for People Who Are Blind or Visually Impaired, 1850 West Roosevelt Road, Chicago, IL 60608-1298, Tel: +1-312-997-3666; Fax: +1-312-506-0104, Gerald.Fishman@chicagolighthouse.org.

The authors have no proprietary or commercial interest in the materials used in this study.

Introduction

Stargardt disease (STGD1, OMIM #248200), first described in 1909 by Karl Stargardt,¹ is the most common form of juvenile-onset hereditary macular dystrophy, with a prevalence of 1:10,000 in the United States and a carrier frequency of about 2%.² It is generally a slowly progressive disease with various phenotypic characteristics and different disease stages. It is most often characterized by central vision loss within the first decades of life that often progresses to the level of legal blindness.³ The hallmark of the disease is the presence of yellowish-white flecks, either limited to the macular region or scattered within the posterior pole, and to a lesser extent, in the mid-peripheral retina.^{1,4}

It is accepted that in patients with macular degeneration, rod sensitivity losses begin earlier and progress more rapidly than cone sensitivity losses based on anatomical and functional measurements.⁵⁻⁷ The greatest losses in rod function occur in the parafoveal region, which extends from 3.5 to 10 degrees from the fovea, which is where rod density is high.⁸ Rod losses have been studied in STGD1 patients with conventional computerized threshold perimetry in a single pilot study that showed rod loss to progress more rapidly than cone losses.⁹

Progress toward therapy for retinal dystrophies is accelerating and clinical trials with the use of novel pharmaceuticals, gene-augmentation therapy, and stem cells are ongoing or planned. Some future therapies are expected to affect rod function, thus making rod-photoreceptor-mediated vision worth measuring to determine the efficacy as well as safety. Recently the MP-1 microperimeter has been modified to perform dark-adapted perimetry.¹⁰ Conventional computerized threshold perimetry measurements rely upon the assumption of foveal fixation, which is lost in the majority of STGD1 patients. An advantage of the MP-1 microperimeter is that it allows a direct view of the fundus image while performing threshold perimetry and accounts for eye movements.¹¹ In the current study we evaluated the usefulness of MP-1S measurements for testing dark-adapted retinal sensitivity in Stargardt patients and compared these findings with structural changes observed by spectral-domain optical coherence tomography (SD-OCT) and confocal scanning laser ophthalmoscope (cSLO) infrared imaging.

Patient and methods

The study included 12 STGD1 patients (mean age 33.4 ± 9.2 yrs) and 10 normally sighted controls (mean age 36.3 ± 15.1 yrs). Patients were diagnosed with Stargardt disease based on the characteristic clinical fundus appearance, clinical history, and genetic analysis (on all but two patients for whom genetic results are pending). The inclusion criteria included STGD1 patients stage I (typically characterized by a localized atrophic appearing foveal lesion surrounded by parafoveal or perifoveal flecks) or II (characterized by retinal flecks throughout the posterior pole, anterior to the vascular arcades and/or nasal to the optic disc),^{12,13} and best-corrected Snellen visual acuity (BCVA) between 20/20 and 20/200. Patients were excluded if they had a refractive error greater than ± 6.0 diopters spherical or ± 2.0 diopters cylindrical, SD-OCT scans of poor quality, evidence of concurrent disease other than STGD1, such as glaucoma, media opacity, uveitis, history of intraocular surgery,

neurologic diseases, diabetes. Patients' demographics, genetics and clinical characteristics are shown in Table 1. All subjects were tested at The Pangere Center for Hereditary Retinal Diseases at The Chicago Lighthouse for People Who Are Blind or Visually Impaired from August 2011 to March 2012. They underwent a comprehensive ophthalmic examination, including visual acuity measurement, refraction, slit-lamp biomicroscopy examination, intraocular pressure measurement with Goldmann tonometry, and dilated direct and indirect fundus examination.

The tenets of the Declaration of Helsinki were followed, and all subjects gave written informed consent after a full explanation of the procedures was provided. Consent procedures were approved by an Institutional Review Board at the University of Illinois at Chicago.

All individuals were scanned using a Spectralis HRA+OCT unit (Heidelberg Engineering, Vista, CA) with the eye-tracking feature. The instrument allows for simultaneous recording of cSLO and SD-OCT images.¹⁴ A minimum standardized imaging protocol was performed in the better-seeing eye of all subjects, which included acquisition of near-infrared reflectance ($\lambda=830\text{nm}$, field of view $30^\circ \times 30^\circ$, image resolution 768×768 pixels) and simultaneous SD-OCT scanning using a second, independent pair of scanning mirrors ($\lambda=870\text{ nm}$, scan depth 1.8 mm, digital depth resolution approximately 3.5 micron per pixel).¹⁵ Because 2 independent pairs of scanning mirrors are used, eye movements are registered and corrected automatically. This allows for pixel-to-pixel correlation of cSLO and SD-OCT findings. A 9-mm line scan along the horizontal meridian, and centered on the fovea, was obtained as an average of 100 scans. The scan from the better-seeing eye of each patient was analyzed.

Dark-adapted microperimetry was performed after 45 minutes of dark adaptation in a darkened room. Microperimetry was repeated twice.

For the first microperimetry test (reference test), cSLO and SD-OCT scans were imported and registered with the MP1-S infrared-fundus image by an automated macular registration, which allowed for precise alignment of the test grid at the fovea. The second test, was performed 5 minutes after the reference test, with the follow-up function of the instrument, in order to test accurately the same points as the reference test. For our measurements a modified MP-1 microperimeter was used to measure dark-adapted thresholds.¹⁰ A 2 log unit neutral density filter and a short-pass filter (150% cutoff =500 nm "blue", Edmund Optics NT52532) were added to the optical path of the instrument. Dark-adapted mean retinal sensitivity (MS) was obtained by using a 37-point grid covering 14° centered on the anatomical fovea, based on SD-OCT scan ($1^\circ=300$ microns, thus $14^\circ=4200$ microns, which encompasses the macular area). Stimulus size was a Goldmann IV and a 4-2 strategy was used. The total examination time and the total effective time (defined as the time it took for the MP1-S to track the fundus and project the point) were recorded for each patient. Examinations longer than 15 minutes were excluded because of their variability from patient fatigue. Pupils were dilated with tropicamide 1% and phenylephrine 2.5%. The non-tested eye was patched with an eye cover during the test. An auto-tracking system calculated the horizontal and vertical shifts in fixation relative to a reference. The MP-1S software includes

an automated tracking system to correct for eye movements. During the examination, eye movements were detected by image acquisition at a rate of 25 frames per second. A computer then calculated the shift between the reference image and the real-time fundus image with the stimulus position on the display corrected according to the actual location of the fundus.

At the conclusion of the examination, the perimetric findings were overlaid onto the cSLO fundus images. The stimulus intensity (the luminance difference between the stimulus and background) ranged from 0.0025 to 0.25 cd/m², a range of 20 dB. Stimulus duration was 40ms. All subjects were exposed to at least ten test spots before the beginning of the examination, to familiarize them with the instrument and minimize the effects of learning on the performance. The test commenced after 45 minutes of dark-adaptation. A super-threshold stimulus was projected onto the blind spot by the machine to monitor false-positive responses. The location of the blind spot was manually identified by the examiner (SS & MAG) before the beginning of the examination as the region over the optic nerve. Any test that produced a false positive was excluded. The spherical equivalent of the patient was added to adjust the clarity of the fixation target and stimuli.

For the spatial assessment of retinal morphological changes, both cSLO and SD-OCT scans were studied simultaneously side by side. This analysis included topographic distribution and signal characteristics of the retinal layers on en face cSLO images over the posterior pole. Fundus reflectivity in cSLO infrared images was defined as hyper-reflective when it appeared qualitatively increased in comparison to controls, as hypo-reflective when it appeared qualitatively decreased in comparison to controls and normally-reflective when it appeared of similar intensity to the controls. Microstructural changes on SD-OCT scans at the retinal pigment epithelium (RPE) reflectance band and photoreceptor cell layers, as well as the inner retinal layers, were evaluated. For the former, individual bands below the hyporeflective band of the outer nuclear layer were analyzed according to Spaide et al¹⁶: (1) a thin hyperreflective band presumed to correspond to the Müller cell junctional complexes of the external limiting membrane, (2) a slightly thicker hyperreflective band corresponding to the inner segment ellipsoid (ISe) band, previously called the inner segment/outer segment border; (3) a thin, only occasionally visible-hyperreflective band presumably corresponding to outer segment/RPE interdigitations, and (4) a broad hyperreflective band that is thought to represent the RPE, Bruch's membrane, and possibly the choriocapillaris.

Data were analyzed and reported as a mean and SD. Student's *t*-test was used for statistical comparisons, with the statistical significance level set to 0.05. Sensitivity was slightly (1.86 dB), but significantly ($p < 0.05$), greater for the first measurement compared to the second, an effect likely attributable to fatigue. Given that the values from the two tests were highly correlated ($r = 0.87$, $p < 0.05$), the values for the two measurements were averaged and all additional analyses were based on this average. However, we also performed the analyses separately and determined that basing analyses on either the first or second measurement instead of the average did not affect any of the conclusions. The mean sensitivity values (dB) for the patients and controls were converted to the percentage difference: $(MS_{cd/m^2} \text{ controls} - MS_{cd/m^2} \text{ patients}) / ((MS_{cd/m^2} \text{ controls} + MS_{cd/m^2} \text{ patients}) / 2) \times 100$.

Results

The Snellen BCVA for the visually normal subjects was 20/20 or better in all examined eyes, whereas the range was 20/20 to 20/200 for the Stargardt patients (Table 1). In STGD patients, ophthalmoscopic lesions were consistent with stage I (small hypopigmented lesion within the fovea with a perifoveal ring of flecks) in all but one patient, who demonstrated more extensive fundus flecks and stage II disease.¹² A foveal scotopic scotoma of 2 log units was identified in visually normal controls on all tests. Figure 1 shows the MP-1S plots for a visually normal control and three representative Stargardt patients. MP-1S measurements indicated that the scotoma was coincident with the foveal centre in all subjects. Mean rod sensitivity \pm SD was 8.34 \pm 1.55 dB for the normal controls and 3.68 \pm 1.74 dB for the Stargardt patients. The difference between the patients and controls was statistically significant ($p<0.001$). The mean sensitivity values (dB) for the patients and controls were converted to the percentage difference. For comparisons based on the percentage difference, there was also a statistically significant reduction in mean rod sensitivity, on average 24.0%, for the Stargardt patients compared to the normal controls ($p<0.001$).

When sensitivity reductions were observed, loss or thinning of the retinal pigment epithelial reflectance band (RPE) on SD-OCT and cSLO infrared images as well as disorganizational loss of the inner segment ellipsoid (ISe),⁶ and external limiting membrane structures on SD-OCT examination were also observed (Figure 1).

All patients exhibited an altered reflectivity on cSLO infrared images, consisting of a normally-reflective region within the fovea surrounded hyporeflectivity. In three patients (patient 4, 5 and 8) a patchy area of hyper-reflectivity could be observed on cSLO infrared images. In this area SD-OCT showed transverse loss of the ISe, ELM and RPE thinning, extending beyond the central hyper-reflective area. MP1S responses superimposed on were found to be 0 dB or non-detectable in the central hyper-reflective area, indicating the presence of a large dense scotoma.

Nonetheless, in some cases scotopic sensitivity loss was observed in the absence of structural changes on SD-OCT and cSLO.

Discussion

The pace of clinical trials in Stargardt disease has been accelerating over the last few years (NCT01367444, NCT01345006, www.clinicaltrials.gov) and several more trials are anticipated. The consequences of visual dysfunction resulting from macular lesions are extremely important to patients' daily living. Measurement of visual function with established methods (e.g. conventional perimetry) remains challenging with Stargardt patients, in fact, the majority of patients have macular lesions that includes foveal degeneration and poor fixation behaviour that complicates the measurement of macular function with conventional perimetry. Retina-tracking microperimetry, is instead independent of the location and stability of fixation because it uses an eye-tracker to obtain psychophysical thresholds and so far has assured accurate correspondence between retinal

structures and visual function.^{11,17} BCVA assessment, although typically used as the gold standard for assessing visual function, is insufficient to fully characterize visual impairment because it is not a specific measure of the photoreceptor function. From a clinical perspective, the assessment of photoreceptor function is a pivotal outcome measure during a trial, regardless of the treatment strategy.

It is the dysfunction and death of photoreceptors that accounts for the vision loss associated with retinal dystrophies. Therefore, photoreceptor health, assessed functionally in a living patient, is the most direct bioassay of the significance of changes in the RPE/Bruch's membrane complex. Degenerative changes in the ISe layer may not be evident by standard imaging techniques, such as SD-OCT and cSLO, until later stages of Stargardt disease. The small cone-dominated fovea, only 0.8 mm (2.75°) in diameter, is surrounded by a rod-dominated parafovea.¹⁸ In young adults, rods outnumber cones in the macula by 9:1. In the entire eye, rods outnumber cones 20:1, so the macula can be considered cone-enriched but not cone-dominated.⁸

The fact that in some cases scotopic sensitivity loss was observed in the absence of structural changes on SD-OCT and cSLO could indicate that photoreceptor dysfunction and early stage degeneration can occur before structural changes are observed with these two methodologies. Our data support the hypothesis that tests of rod function will permit detection of early dysfunction. Probably, as in the normal aging process,¹⁸ in STGD1 patients the rod numbers at a precise location decrease with the pathological process, but the outer segments of individual remaining rods produce a compensatory hypertrophy that explains why the ISe may appear normal in SD-OCT in the presence of a reduction of dark-adapted function. Rod photoreceptors not only serve as an early indicator of impending cone dysfunction, but they also contribute in important ways to daily visual behavior. An early intervention may not only rescue degenerating rods, but also indirectly contribute to the preservation of cones, since rods produce a diffusible substance essential for cone survival.¹⁹

To the best of our knowledge this is the first study of dark-adapted sensitivity with MP1S in STGD1 patients. Crossland et al. first introduced the instrument in 2011¹⁰ and Birch et al. studied rod sensitivity in patients with cone dystrophy and retinitis pigmentosa.²⁰ In this study we found that the use of a MP-1S can adequately measure dark-adapted retinal sensitivity in visually normal controls and STGD1 patients. Those with Stargardt disease showed a significant loss in scotopic mean retinal sensitivity compared to normally sighted controls that was associated with structural changes of the retina.

In both STGD1 patients and normal controls we did not find a large range in retinal sensitivity values, likely due to the low dynamic stimulus range of the MP-1S LCD display, that operates over only a 2 log unit luminance range. As a consequence, some subjects (for example Stargardt patient 5, table 1) were able to identify the dimmest stimulus that can be presented with the MP-1S (shown as filled green square in Figure 1), meaning that dimmer stimuli would have been required in order to accurately measure sensitivity. Future measurement devices will need to extend the dynamic range of the microperimeter.

Nonetheless, the currently modified MP-1S microperimeter can depict, with topographical accuracy, changes in scotopic sensitivity in Stargardt patients.

Macular retina is consistently involved in all stages of Stargardt dystrophies and AMD and new technologies of cross-sectional imaging, autofluorescence, infrared fundus imaging and adaptive optics are providing detailed information on the anatomical/structural changes occurring at the level of photoreceptors and the RPE of the macular region.²¹ The novel findings of this study have wide-reaching application in the diagnosis of retinal disease and the monitoring of disease progression. Restoration of vision is the ultimate goal of research on retinal degeneration and gene therapy is a promising field of research. However, in gene therapy, the rate of success depends on the amount of photoreceptors still preserved. The ability to identify and target retinal locations with retained photoreceptors function is a prerequisite for successful gene therapy, hence MPIS can be useful for the determination of the most optimal areas for future treatment and provide valuable information on the natural history for scotopic visual loss in patients with Stargardt disease and other related retinal diseases.

Acknowledgments

Financial Support: Pangere Corporation; The Chicago Lighthouse for People who are Blind or Visually Impaired; National Institute of Health grant R00EY019510 (JJM)

References

1. Stargardt, K. Albrecht von Graefes Arch Klin Exp Ophthalmol. 1909. Über familiäre progressive Degeneration in der Makulagegend des Auges; p. 534-550.
2. Blackarski, P. Fundus Flavimaculatus. Retinal dystrophies and Degenerations. New York: Raven Press; 1988. p. 135-159.
3. Rotenstreich Y, Fishman GA, Anderson RJ. Visual acuity loss and clinical observations in a large series of patients with stargardt disease. Ophthalmology. 2003; 110(6):1151–1158.10.1016/S0161-6420(03)00333-6 [PubMed: 12799240]
4. Fishman GA. Fundus flavimaculatus. A clinical classification. 1976; 94(12):2061–2067.
5. Scholl HPN, Bellmann C, Dandekar SS, Bird AC, Fitzke FW. Photopic and scotopic fine matrix mapping of retinal areas of increased fundus autofluorescence in patients with age-related maculopathy. Investigative Ophthalmology & Visual Science. 2004; 45(2):574–583. [PubMed: 14744901]
6. Curcio CA, Medeiros NE, Millican CL. Photoreceptor loss in age-related macular degeneration. Investigative Ophthalmology & Visual Science. 1996; 37(7):1236–1249. [PubMed: 8641827]
7. Owsley C, McGwin G Jr, Jackson GR, Kallies K, Clark M. Cone- and Rod-Mediated Dark Adaptation Impairment in Age-Related Maculopathy. Ophthalmology. 2007; 114(9):1728–1735.10.1016/j.ophtha.2006.12.023 [PubMed: 17822978]
8. Curcio CA, Owsley C, Jackson GR. Spare the rods, save the cones in aging and age-related maculopathy. Investigative Ophthalmology & Visual Science. 2000; 41(8):2015–2018. [PubMed: 10892836]
9. Cideciyan AV, Swider M, Aleman TS, et al. ABCA4 disease progression and a proposed strategy for gene therapy. Human Molecular Genetics. 2009; 18(5):931–941.10.1093/hmg/ddn421 [PubMed: 19074458]
10. Crossland MD, Luong VA, Rubin GS, Fitzke FW. Retinal specific measurement of dark-adapted visual function: validation of a modified microperimeter. BMC Ophthalmol. 2011; 11(1): 5.10.1186/1471-2415-11-5 [PubMed: 21303544]

11. Sawa M, Gomi F, Toyoda A, Ikuno Y, Fujikado T, Tano Y. A Microperimeter That Provides Fixation Pattern and Retinal Sensitivity Measurement. *Jpn J Ophthalmol.* 2006; 50(2):111–115.10.1007/s10384-005-0292-y [PubMed: 16604385]
12. Fishman GA, Stone EM, Grover S, Derlacki DJ, Haines HL, Hockey RR. Variation of clinical expression in patients with Stargardt dystrophy and sequence variations in the ABCR gene. *Arch Ophthalmol.* 1999; 117(4):504–510. [PubMed: 10206579]
13. Genead MA, Fishman GA, Stone EM, Allikmets R. The Natural History of Stargardt Disease with Specific Sequence Mutation in the ABCA4 Gene. *Investigative Ophthalmology & Visual Science.* 2009; 50(12):5867–5871.10.1167/iovs.09-3611 [PubMed: 19578016]
14. Helb H-M, Issa PC, Fleckenstein M, et al. Clinical evaluation of simultaneous confocal scanning laser ophthalmoscopy imaging combined with high-resolution, spectral-domain optical coherence tomography. *Acta Ophthalmologica.* 2010; 88(8):842–849.10.1111/j.1755-3768.2009.01602.x [PubMed: 19706019]
15. Fleckenstein M, Issa PC, Helb HM, et al. High-Resolution Spectral Domain-OCT Imaging in Geographic Atrophy Associated with Age-Related Macular Degeneration. *Investigative Ophthalmology & Visual Science.* 2008; 49(9):4137–4144.10.1167/iovs.08-1967 [PubMed: 18487363]
16. Spaide RF, Curcio CA. Anatomical correlates to the bands seen in the outer retina by optical coherence tomography: literature review and model. *Retina (Philadelphia, Pa).* 2011; 31(8):1609–1619.10.1097/IAE.0b013e3182247535
17. Issa PC, Helb HM, Rohrschneider K, Holz FG, Scholl HPN. Microperimetric Assessment of Patients with Type 2 Idiopathic Macular Telangiectasia. *Investigative Ophthalmology & Visual Science.* 2007; 48(8):3788–3795.10.1167/iovs.06-1272 [PubMed: 17652753]
18. Curcio CA, Millican CL, Allen KA, Kalina RE. Aging of the human photoreceptor mosaic: evidence for selective vulnerability of rods in central retina. *Investigative Ophthalmology & Visual Science.* 1993; 34(12):3278–3296. [PubMed: 8225863]
19. Hicks D, Sahel J. The implications of rod-dependent cone survival for basic and clinical research. *Investigative Ophthalmology & Visual Science.* 1999; 40(13):3071–3074. [PubMed: 10586925]
20. Birch DG, Wen Y, Locke K, Hood DC. Rod Sensitivity, Cone Sensitivity, and Photoreceptor Layer Thickness in Retinal Degenerative Diseases. *Investigative Ophthalmology & Visual Science.* 2011; 52(10):7141–7147.10.1167/iovs.11-7509 [PubMed: 21810977]
21. Chen Y, Ratnam K, Sundquist SM, et al. Cone Photoreceptor Abnormalities Correlate with Vision Loss in Patients with Stargardt Disease. *Investigative Ophthalmology & Visual Science.* 2011; 52(6):3281–3292.10.1167/iovs.10-6538 [PubMed: 21296825]

Summary statement

Dark-adapted retinal sensitivity, measured by a modified MP-1 microperimeter (MP-1S), was found to be associated with structural changes determined by spectral-domain optical coherence tomography and confocal scanning laser ophthalmoscope infrared fundus imaging. Associating functional loss with structural changes will be useful for patient monitoring in future clinical trials.

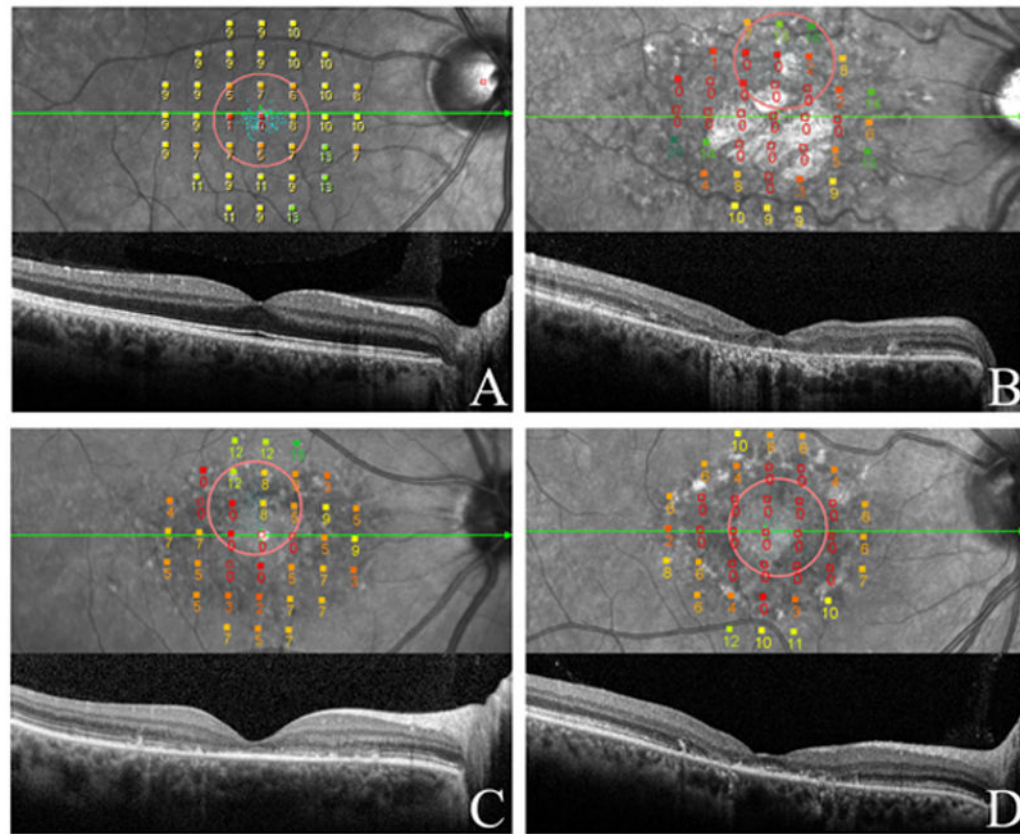


Figure 1.

Dark-adapted fundus related perimetry superimposed on the cSLO image and corresponding SD-OCT of a normally sighted subject (A) and Stargardt patients (B,C,D).

Numbers represent sensitivity (dB) at each point tested and colors classify sensitivity (bright green shows best function, deep red shows poorest function).

The green arrow indicates the direction of the SD-OCT scan included directly below. The red circle indicates the fixation target.

(A) Horizontal SD-OCT scan through the macula shows normal retinal structure and thickness. Scotopic mean retinal sensitivity was 11 dB. Fixation was predominantly central and stable.

(B) SD-OCT shows thinning of the RPE, loss of the ISe and thinning of the outer nuclear layer (ONL). Scotopic mean retinal sensitivity was 4.7 dB. Fixation was predominantly eccentric, located in the superior hemiretinal region, and “relatively unstable.”

(C) Disorganizational loss of the ISe and external limiting membrane on SD-OCT correlates with loss of retinal sensitivity. Scotopic sensitivity was 5.2 dB, while fixation was predominantly eccentric, located in the superior hemiretinal region, and “relatively unstable.”

(D) RPE thinning and ISe loss with foveal sparing on the SD-OCT. Retinal sensitivity was 3.6 dB, fixation was “poor central” and “relatively unstable.”



Figure 2. cSLO infrared images (A,C) and corresponding SD-OCT scans (B,D) of patient 3 (A,B) and patient 6 (C,D). The white arrows indicate the direction of the SD-OCT scans. SD-OCT show ISe disorganization in the fovea with normal appearing outer nuclear layer and RPE layers, and normal ISe outside the foveola. The numbers in the box show dark-adapted sensitivity results (expressed in dB) corresponding to those areas. Scotopic sensitivity loss (4,5,6 dB) was observed in the absence of structural changes on SD-OCT and cSLO (B,D).

Table 1

Age, Race, Visual Acuity and Genetic Mutations in Stargardt Patients
Patients' demographics, genetics and clinical characteristics

Patient Number/Gender (F/M)	age	race	BCVA	Mutation	Stage	MS (dB)
1/F	33	Asian	20/80-2	gly1961glu exon 42 and IVS2+2T>C; compound heterozygous	I	6.3
2/F	25	White	20/200	leu514pro exon 12, ala1038val exon 21& 11846 T exon 39; compound heterozygous	I	3.05
3/M	47	White	20/30-1	gly1961glu exon 42, homozygous and thr1253met exon 21; heterozygous	I	5.4
4/F	37	White	20/200	trp1408arg; heterozygous	I	1.65
5/M	36	White	20/25+2	leu541pro exon 12, ala1038val exon 21; compound heterozygous	I	5.45
6/F	23	White	20/20+2	gly863Ala and Arg219Thr; compound heterozygous	I	4.8
7/M	20	White	20/30+1	gly863Ala and Arg219Thr; compound heterozygous	I	3.55
8/F	40	AfroAmerican	20/25-1	Results pending	I	3.1
9/F	28	White	20/40	leu541pro exon 12, ala1038val exon 21; compound heterozygous	I	0.6
10/F	29	White	20/20	Results pending	I	2.2
11/F	50	AfroAmerican	20/30	leu1201arg exon 24 & gly1961glu exon 42; compound heterozygous.	I	5.15
12/M	33	White	20/200+1	arg1898his exon 40 and lys 2056stop exon45; compound heterozygous	II	2.95

F: Female, M: Male, BCVA: Best Corrected Visual Acuity, MS: mean dark-adapted retinal sensitivity